A Rotor Circulation near the Baiu Front Observed by the MU Radar[1]

By Akira Watanabe

Faculty of Education, Fukushima University, Fukushima 960-12, Japan

Shoichiro Fukao, Manabu D. Yamanaka

Radio Atmospheric Science Center, Kyoto University, Uji, Kyoto 611, Japan

Akimasa Sumi

Center for Climate System Research, University of Tokyo, Tokyo 153, Japan

and

Hiroshi Uyeda

Department of Geophysics, Hokkaido University, Sapporo 060, Japan

(Manuscript received 31 March 1993, in revised form 29 September 1993)

Abstract

A rotor circulation was directly observed near the Baiu front in the lower troposphere by three-dimensional Döppler measurements with the MU radar at Shigaraki, Japan (35°N, 136°E). The temporal and vertical scale of the rotor were $\sim$50 min and $\sim$2 km, and the stratification observed by radiosondes was statically stable. The synoptic meteorological analysis suggests that the rotor existed just below and between Baiu-frontal banded precipitation clouds which were organized in a meso-α-scale cyclone. Precipitation echoes observed simultaneously by C/Ku-band radars were quite weak in the downdraft in front of the rotor, and became significant and tall up to $\sim$9 km altitude at the back of the rotor circulation. The rotor was identified with a meso-β-scale depression observed by the routine meteorological network, which had a horizontal scale of $\sim$40 km in the zonal direction and 150–200 km in the meridional direction, and moved from west to east at $\sim$50 km/h. Based on brief discussions, we conclude that the rotor circulation was locally developed from an orographic disturbance by shear instability which was occasionally induced in a weak statically-stable layer maintained by (conditional) symmetric instability.

1. Introduction

Rotor circulations in the lower troposphere have been a subject mainly related to turbulence, gravity waves and billow (or lenticular) clouds generated on the leeward side of mountains. Förchtgött (1949) classified types of the airflows over ridges, and pointed out that generation of a rotor circulation is determined mainly by the shape of the wind profile. Larsson (1954) described the frequent appearance of lenticular clouds in a layer of wind exceeding 15 m/s at 4–7 km altitude above rotor circulations. Gerbier and Berenger (1961) proposed a schematic model of lee-side gravity wave structure including rotor circulations with the center and size governed by a mountain range. Bretherton (1969) reviewed the theory of vertical transport of horizontal momentum by lee wave phenomena, and Lilly (1971) measured the lee wave stress using instrumented aircraft flying through a lee wave structure. However, those investigations have never directly detected the three-dimensional wind velocity field associated with a rotor circulation.

In this paper, we present a rotor circulation detected near the Baiu front by the MU radar located

[1]Extended from a paper presented at the Fifth Workshop on Technical and Scientific Aspects of MST Radar, Aberystwyth, Wales, UK, 6–9 August 1991.

at Shigaraki, Japan (34.85°N, 136.10°E, and 375 m altitude above the mean sea level) which can observe the three-dimensional wind velocity with high resolutions (~1 min and ~150 m) in time and height (see Fukao *et al.*, 1985b, c, 1988, 1991). This is the first direct observation of this kind, as far as we know. The thermodynamical and cloud-physical features were simultaneously observed by using radiosondes and C/Ku-band radars at the MU radar site. The synoptic- and meso-scale horizontal structures are also studied based on the routine meteorological network of Japan Meteorological Agency (JMA). We consider briefly the mechanism generating this circulation and the significance in the Baiu-frontal atmosphere.

2. Synoptic-scale situation

The rotor circulation reported in this paper was observed around the midnight during July 2–3, 1990. We use Japanese Standard Time (JST) throughout this paper. Prior to a description of the evidence of a rotor circulation itself, we shall describe the synoptic-scale situations obtained from routine observations by JMA at ~21 JST on July 2.

As shown in Fig. 1a, the Baiu front at the surface was located across west Japan, and a medium- (or meso-α-) scale cyclone was approaching from the Korean Peninsula to the west of Japan. This cyclone had been changed from a typhoon (T9006, Percy) over the Chinese Continent on June 30, and was accompanied with a number of banded clouds within the distance of ~1000 km from the cyclone center (see Fig. 1b). It must be noted that banded clouds existed along approximately NNW–SSE directions over central Japan, including the location of the MU radar observatory. A high relative humidity area corresponding to these banded clouds existed approximately above the frontal surface.

The front at the ground had a warm-front-like feature to the south of the MU radar observatory, and the frontal surface located at 3–5 km altitude over the observatory (see Fig. 2). This front moved northeastward very slowly, and became an occluded front in the daytime on July 3. The occluded front at the ground passed by the observatory on July 5, and striking precipitations (5–10 mm/h) were observed there mainly during July 3–4, although these phenomena will be reported in a subsequent paper by our group.

Easterly wind (~10 m/s) exists below the frontal surface over central Japan, whereas a westerly wind dominates above the frontal surface. Wind speed is stronger near the frontal surface, and a weak low-level jet stream (~15 m/s) exists at ~700 hPa or ~3 km altitude over ~33°N. Cold and wet air below the frontal surface induces a strong shear near the frontal surface through the thermal-wind balance. These are not far-from-common features known in the Baiu-frontal atmosphere (Matsumoto *et al.*, 1971; Akiyama, 1973; Ninomiya and Akiyama, 1974), but here we must note that the vertical shear becomes strong near the frontal surface, in particular over central Japan including the location of the MU radar observatory.

3. Observations at the MU radar observatory

3.1 MU radar observations

We observed two height ranges of 1–14 km and of 5–20 km alternately by the MU radar, and obtained vertical profiles of the three-dimensional wind velocity components in the lower troposphere at about 2 min intervals. Details of the MU radar system has been given in Fukao *et al.* (1985b, c, 1988), and the observational technique used here is a standard one as described in Fukao *et al.* (1989, 1991), May *et al.* (1992) and Kotani *et al.* (1993). In estimating the wind velocity from the MU radar echo data, the raindrop echoes were omitted, following earlier studies by Fukao *et al.* (1985a), Wakasugi *et al.* (1986) and T. Sato *et al.* (1990). Although the MU radar echoes from a height lower than 2 km are often distorted by the recovery effect of the receiver, the wind velocity data upper than 1.2 km are reliable in this observational period.

The zonal, meridional and vertical velocities (u, v, w) observed by the MU radar are shown in Fig. 3. The highlight of this paper appears in Fig. 3a; where a clear rotor circulation appears in the u-w flow field in a height range of 1–3 km during 0015–0105 JST on July 3. Namely, the rotor center is located at ~2 km height above the ground (about 2.4 km altitude above the mean sea level), and the vertical size of the rotor is ~2 km. The time scale relative to the ground is ~50 min. However, we cannot find such a clear circulation pattern in the v-w flow field (see Fig. 3b), which implies that the rotor axis is approximately along the meridional direction. A weak wavy structure with time scale similar to the rotor is found, but this is almost certainly due to the variations of w associated with the rotor circulation mentioned above. There are no striking variations for v (unlike u) in the height range of the rotor. Although the MU radar observations were carried out over five days (2–6 July 1990), we did not observe any such clear rotor circulation other than that mentioned above.

The MU radar data are plotted in another way in Fig. 4. In the u-v field shown in Fig. 4a, we find that a southeasterly wind of about 18 m/s is predominant from 1.5 to 2 km above the ground, while a southwesterly wind predominates from 2 to 3 km and a westerly (or northwesterly) wind of about 13 m/s predominates above 3 or 4 km. When the southwesterly wind region becomes thin, the rotor occurs in the region. The westerly wind just above the rotor circulation corresponds to the Baiu-frontal low-level

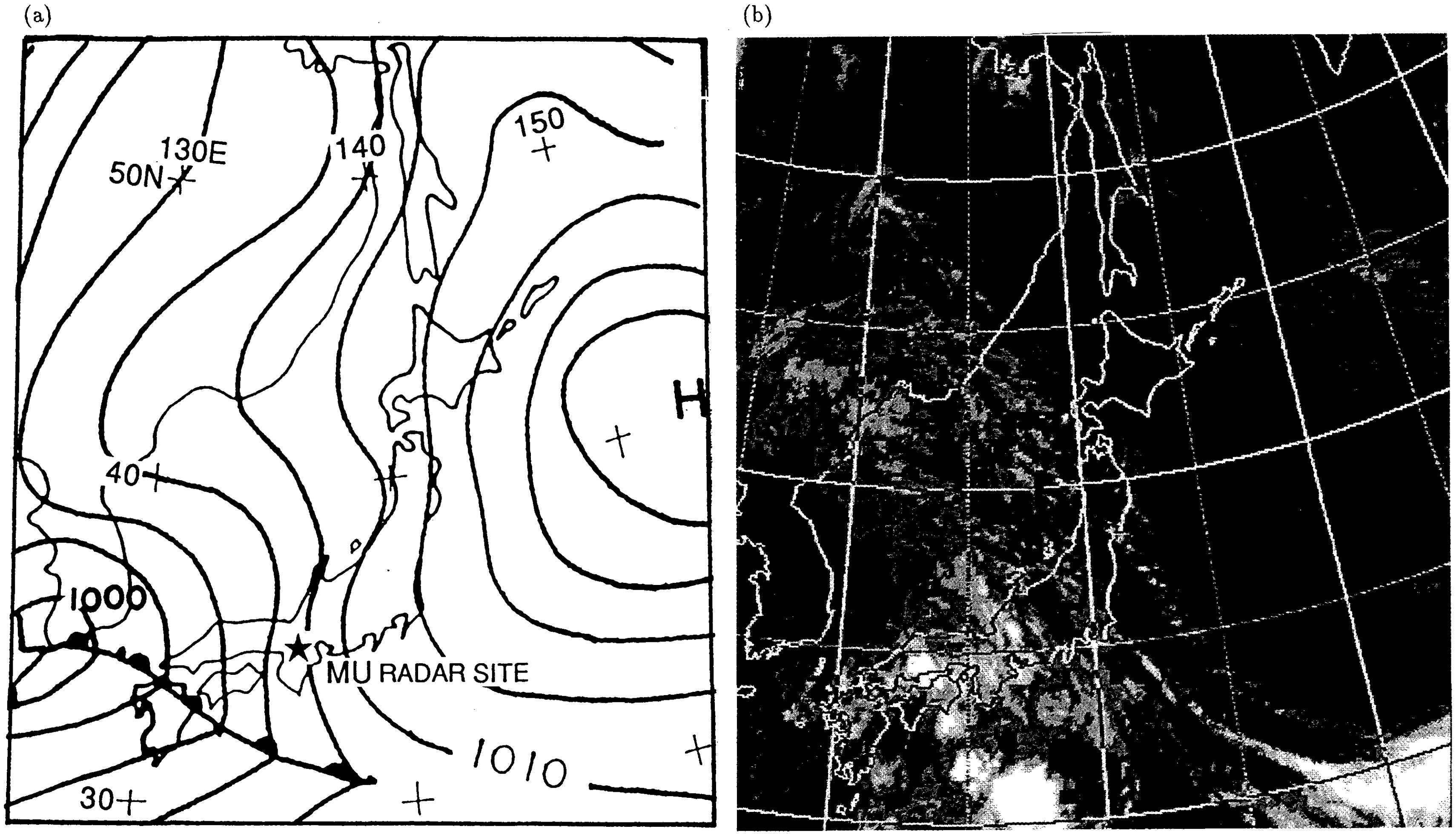

Fig. 1. (a) Surface synoptic map at 21 JST (12 UT) on July 2, 1990 and (b) GMS IR image at 00 JST on July 3 (15 UT on July 2), 1990 transcribed directly from the routine products of the Japan Meteorological Agency (JMA).

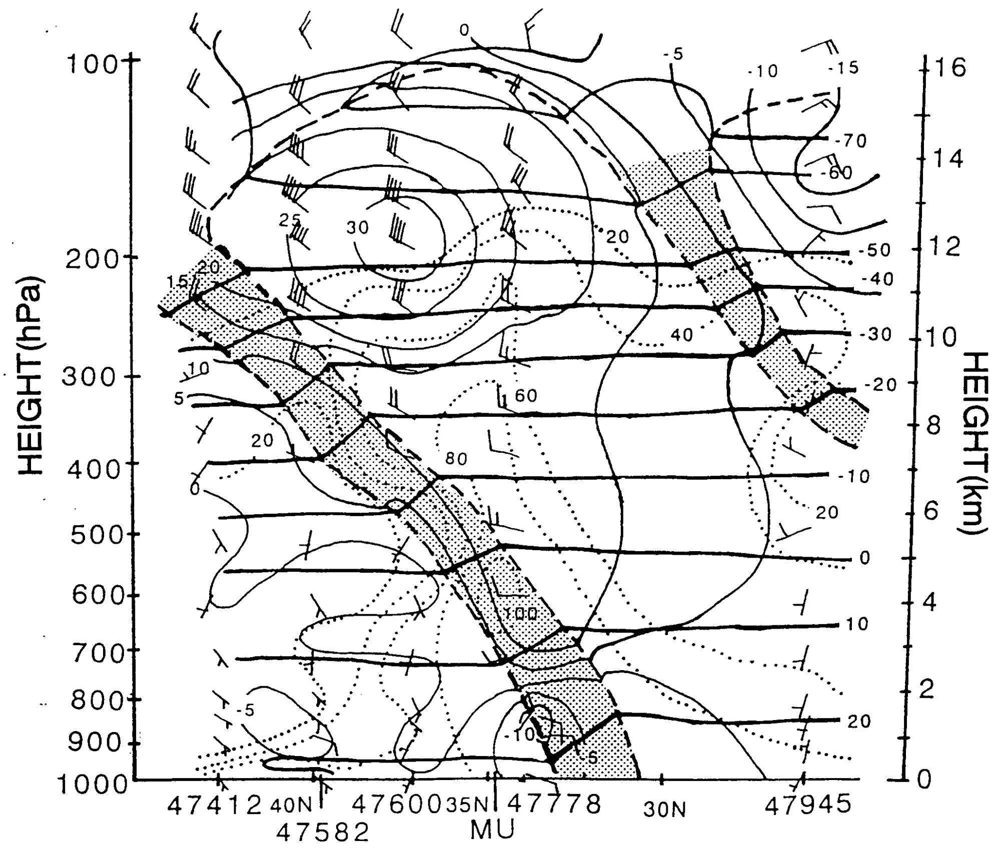

Fig. 2. Quasi-meridional cross-section at 21 JST (12 UT) on July 2, 1990 of temperature (thicker solid contours, every 10°C), zonal wind velocity (thinner solid contours, every 5 m/s), relative humidity (dotted contours, every 20 %) and the tropopause and frontal surface (thick dashed curves), based on observations at the MU radar observatory (34.85°N, 136.10°E) and five JMA stations located along an approximately NNE-SSW line passing through the central Japan (a map was given in Fukao *et al.*, 1988; Larsen *et al.*, 1991): of Sapporo (47412), Akita (47582), Wajima (47600), Shionomisaki (47778) and Minamidaitojima (47945). Pressure is taken as the vertical coordinate (the ordinate), and altitude plotted in the right-hand side axis is correct at Shionomisaki. Total horizontal winds at standard pressure levels over the JMA stations are also indicated by short (5 m/s) and long (10 m/s) barbs.

jet stream mentioned in Section 2, and the easterly below the rotor seems somewhat stronger than that analyzed in Fig. 2. The vertical shear of horizontal wind velocity ($\partial u/\partial z$, $\partial v/\partial z$) becomes large in the region between the southeasterly wind in the lower layer and the northwesterly wind in the upper layer. On the other hand, in Fig. 4b, there appears an updraft above and behind the rotor center, while a downdraft appears in front of it. Another weak downdraft is seen at 1–2 km altitude after 0100 JST, but we can barely discern another rotor circulation pattern.

The echo power intensity of the MU radar in the case of no precipitation is useful as a measure of microscale turbulence activity (or stratification stability), and is used sometimes for estimating the tropopause and frontal surfaces (see Fukao *et al.*, 1988, 1989; Kotani *et al.*, 1993). However, in the period and region of appearance of the rotor circulation, the echo power intensity data did not clearly indicate such strong turbulence as is expected in a statically (or convective) instability appearing near a very active frontal surface. Furthermore some special observations using velocity-azimuth display (VAD) methods (Fukao *et al.*, 1988; Larsen *et al.*, 1991) and interferometry techniques (Palmer *et al.*, 1991) have shown that the vertical velocity measured as the Döppler velocity of the MU radar vertical beam may be modified by a significant non-vertical refraction by layered turbulence with a small inclination (sufficiently less than the beam half-width ~3.6°). However, there was no striking turbulence including inclined layered turbulence causing such a modification, and we can safely state that the vertical velocity shown in Figs. 3 and 4 is farely reliable.

3.2 Radiosonde observations

The vertical profiles of temperature and humidity were observed by using a standard radiosonde

(a)

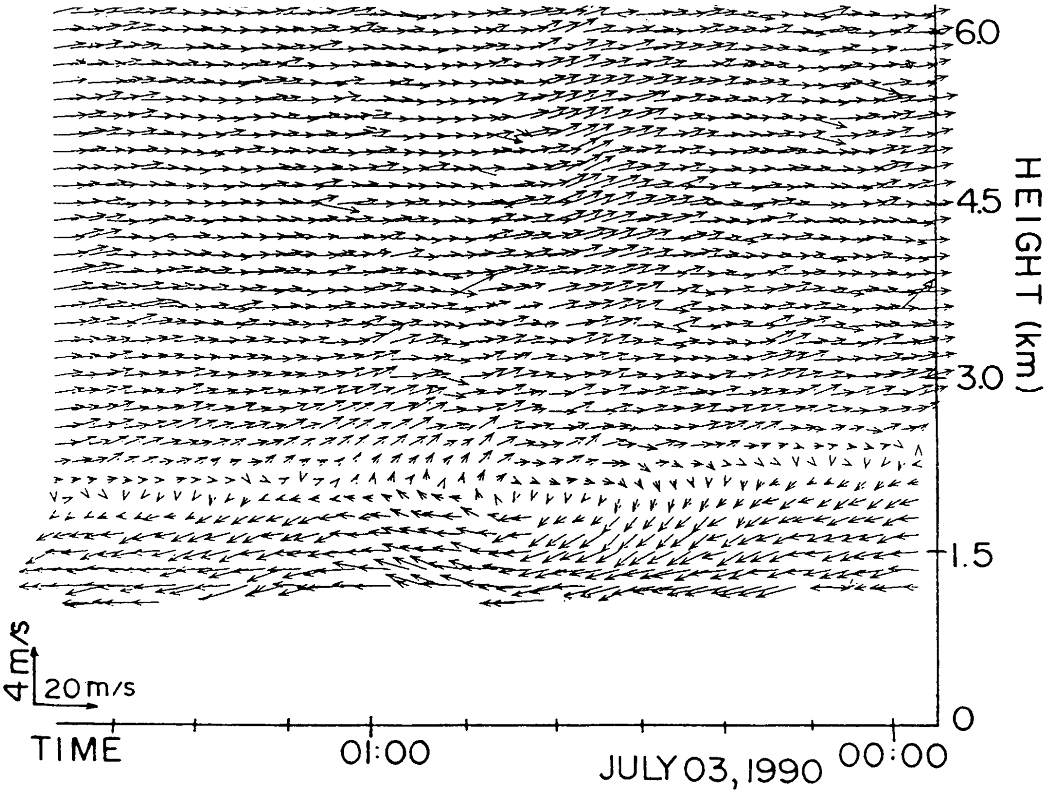

(b)

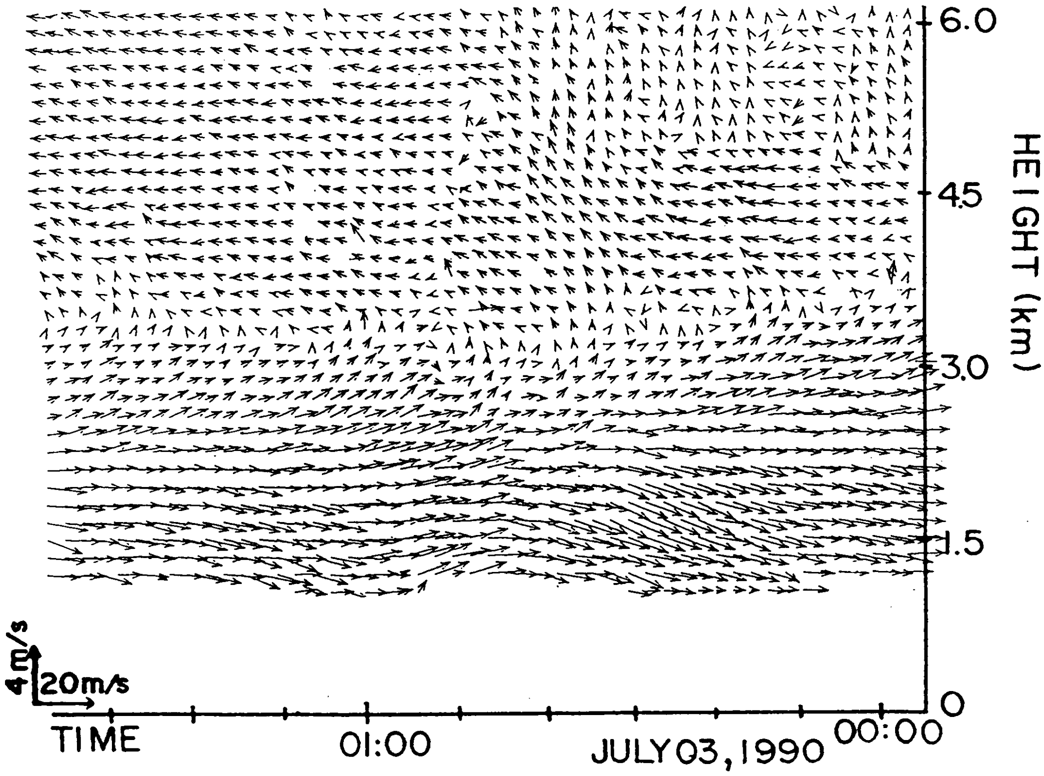

Fig. 3. (a) Zonal-vertical (eastward and upward positive) and (b) meridional-vertical (northward and upward positive) air flows observed by the MU radar from 2357 JST on July 2 to 0136 JST on July 3, 1990. Time resolution is approximately 2.5 minutes.

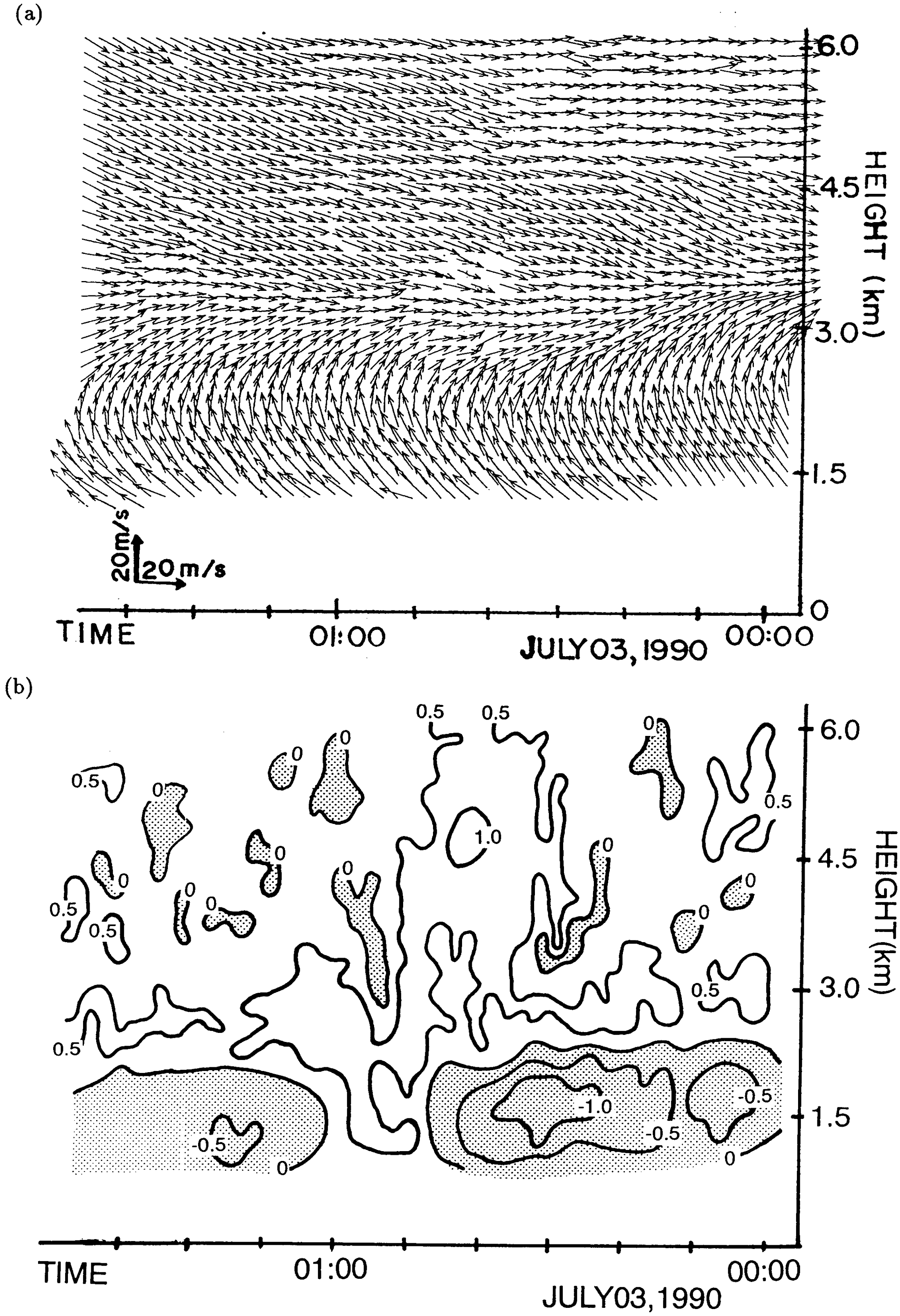

Fig. 4. (a) Zonal-meridional (eastward and northward positive) and (b) vertical (upward positive) air flows observed by the MU radar from 2357 JST on July 2 to 0136 JST on July 3, 1990. Time resolution is approximately 2.5 minutes.

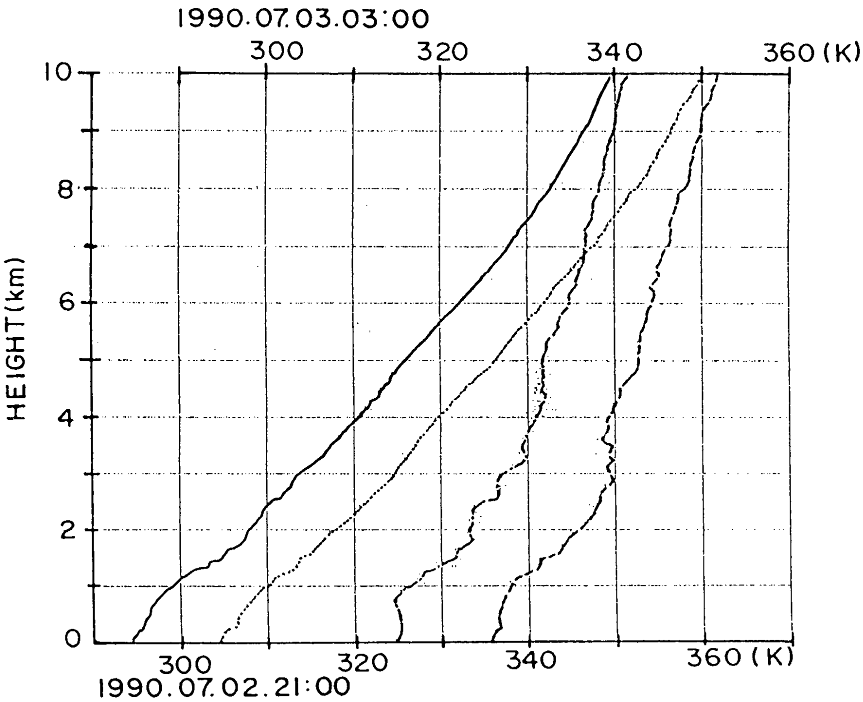

Fig. 5. Vertical profiles of potential temperature (—— 21 JST on July 2; ··· 03 JST on July 3, 1990) and equivalent potential temperature (-·-·- 21 JST on July 2; - - - 03 JST on July 3, 1990), observed with radiosondes launched at the MU radar observatory. The data of 03 JST on July 3 are displaced by 10 K.

system (VAISALA RS80) launched from the MU radar observatory before (21 JST on July 2) and after (03 JST on July 3) the appearance of the rotor circulation. Figure 5 shows vertical profiles of potential temperature (θ) and equivalent potential temperature (θ_e) calculated from the results of these radiosonde observations. We find that $\theta_e \approx 325\,\mathrm{K}$ below $\sim$1 km altitude and $\theta_e \approx 340\,\mathrm{K}$ above $\sim$3 km altitude. This layer of strong static stability (large θ_e-gradient) is identified with the altitude range of the rotor circulation seen in Fig. 3a and also approximately with the frontal surface shown in Fig. 2.

Both θ and θ_e profiles do not suggest any statically unstable layer with the vertical scale of the rotor circulation ($\sim$2 km). This result is consistent with the observational features for the MU radar echo power intensity mentioned before. Before the rotor appears, the planetary boundary layer below 1 km height seems almost neutral, but the height region in which the rotor is to appear is statically stable. After the rotor appears, both the height regions become more stable. The thickness between the levels of $\theta_e = 335\,\mathrm{K}$ and 340 K is increased from 1.2 to 2.4 km before and after the rotor, which seems consistent with moist warm air advection associated with the southwesterly seen in the same height range in Fig. 4a.

Figure 6 shows the distribution of the (equivalent) Richardson number (for wet atmosphere)

$$Ri \equiv \frac{g}{\theta_e}\frac{\partial \theta_e}{\partial z}\left[\left(\frac{\partial u}{\partial z}\right)^2 + \left(\frac{\partial v}{\partial z}\right)^2\right]^{-1}$$

calculated from 10-min-averaged u and v observed by the MU radar and θ_e interpolated from the double radiosonde measurements mentioned above. It took about 20 min for a radiosonde balloon to pass the 6 km height after the launch, and this time lag has been considered in the analysis of Fig. 6. It should be noted that Ri calculated here is not of the background field but affected by the disturbed wind field including the rotor circulation itself. However, we find $Ri < 1$ (suggesting symmetric instability) in a region broader than that of the rotor circulation, and $Ri < 1/4$ (suggesting shear instability) at the rotor center. These results imply that the rotor circulation is generated by symmetric and/or shear instabilities in a statically stable layer just near the Baiu-frontal surface; this will be discussed in Section 5.

3.3 C/Ku-band radar observations

At the MU radar observatory, two separate antennas of C (5.265 GHz) and Ku (13.85 GHz) bands fixed pointing vertically measured the vertical structure of precipitation echoes. A detailed description of the C/Ku-band radars has been given in Fukao *et al.* (1985a).

As shown in Fig. 7, the echo power of the Ku-band radar becomes weaker in the region near the rotor

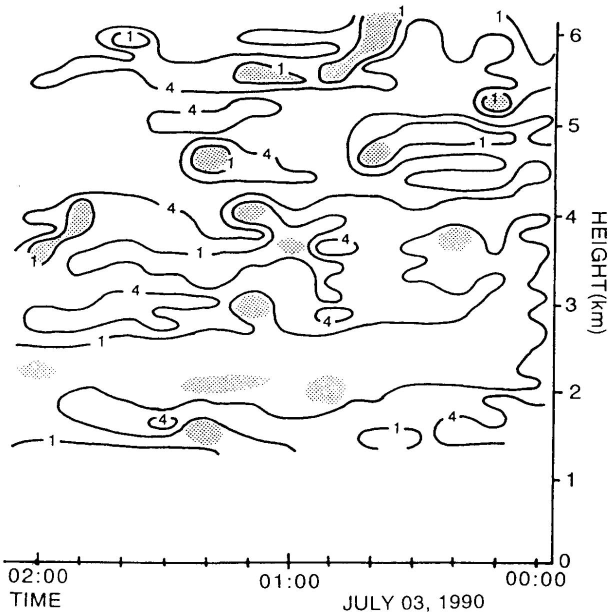

Fig. 6. Distribution of the Richardson number (for wet air) calculated using the horizontal wind obtained from 10-min-averaged MU radar data and equivalent potential temperature interpolated from the observations by radiosondes launched at ~21 JST on July 2 and at ~03 JST on July 3, 1990 (with correcting the time lags of balloons passing each altitude). The regions of values less than 1/4 are shaded.

circulation (00–01 JST on July 3; 1–4 km height), and disappears in the downdraft in front of the rotor. On the other hand, the echo power is significant, extending up to 9 km in height behind the rotor circulation. Similar results were also obtained by the C-band radar, and raindrop echoes before and after the rotor circulation were also detected by the MU radar. The bright band (or precipitation melting layer) was observed at around 4 km height, which is just lower than the freezing (0°C) level existing at ~5 km altitude (~4.6 km height above the ground of the MU radar observatory) seen in Fig. 2. According to cloud-physical studies (*e.g.*, Takeda and Fujiyoshi, 1978; Matsuo and Sasyo, 1981; Yokoyama *et al.*, 1984, 1985), a melting layer generated at a distance of ~10^2 m below the freezing level is consistent with the relative humidity of ≤ 90 % near the freezing level observed by radiosondes.

The tall echoes observed behind the rotor (and also 1–3 h earlier than the rotor) are considered corresponding to banded clouds seen in Fig. 1b. The features of intermittent and trail-like appearance of those echoes in the middle and upper troposphere are quite similar to the generating cells observed in various warm-frontal precipitations (*e.g.*, Browning *et al.*, 1973; Hobbs, 1978; Takeda and Horiguchi, 1986). Similar situations have been considered also in the Baiu-frontal banded areas of heavy precipitation (*cf.* Ninomiya and Akiyama, 1974; Akiyama, 1978). In this case the frontal surface (expected to be at the bottom of the generating cells) was lower than the melting layer, so that the seeder-feeder mechanism (activating precipitation by ice crystals generated in and falling from the generating cells) could hardly work. The precipitation intensity observed at the MU radar observatory during the night of July 2–3 was not strong (< 3 mm/h). The banded clouds and precipitation will be discussed again in the next section.

4. Mesoscale horizontal structure

In order to study the horizontal structure of the rotor circulation observed in Section 3, we use the data provided by the Osaka Meteorological Observatory (OMO) of JMA.

Figure 8 shows distributions of raindrop echoes observed by a standard meteorological radar (C-band, 5.30 GHz) of OMO at 0015, 0045 and 0100 JST on July 3. In the echo distribution at 0045 JST (see the middle panel) the MU radar is located near the western boundary of a meso-β-scale clear region elongated in the north-south direction between two rainfall regions. This feature suggests that the downdraft region (former or eastern half) of the rotor circulation corresponds approximately to the western half of this clear region, which is consistent also with the banded clouds seen in the satellite imagery (Fig. 1b) and the C/Ku band radar observations (Fig. 7). The clear region has a size of 150–200 km in the meridional direction and ~40 km in the zonal direction. Thus the size of the rotor is considered to be similar to that of the clear region described here.

We find that the clear region discussed above is less distinct in the raindrop echo distributions at 0015 and 0100 JST (see the left and right panels of Fig. 8). We can roughly estimate the movement of the clear region as ~50 km/h eastward, which is close to the low-level jet stream (≈15 m/s) located at ~3 km height. Considering that the rotor circulation moves eastward with this speed, we obtain a consistent result for the size of the rotor circulation (observed for ~50 min in Fig. 3a) as ~40 km in the zonal direction. The indistinct features of the clear region before and after the rotor event imply that the rotor circulation is generated by a special situation in a limited period and area (see Section 5). Indeed, in spite of the existence of many similar banded clouds in Fig. 1b, we do not find another clear region of similar size and shape in Fig. 8; this is consistent with the fact that we can barely discern another distinct rotor circulation in the MU radar observations shown in Fig. 3.

Temporal changes of surface pressure and temper-

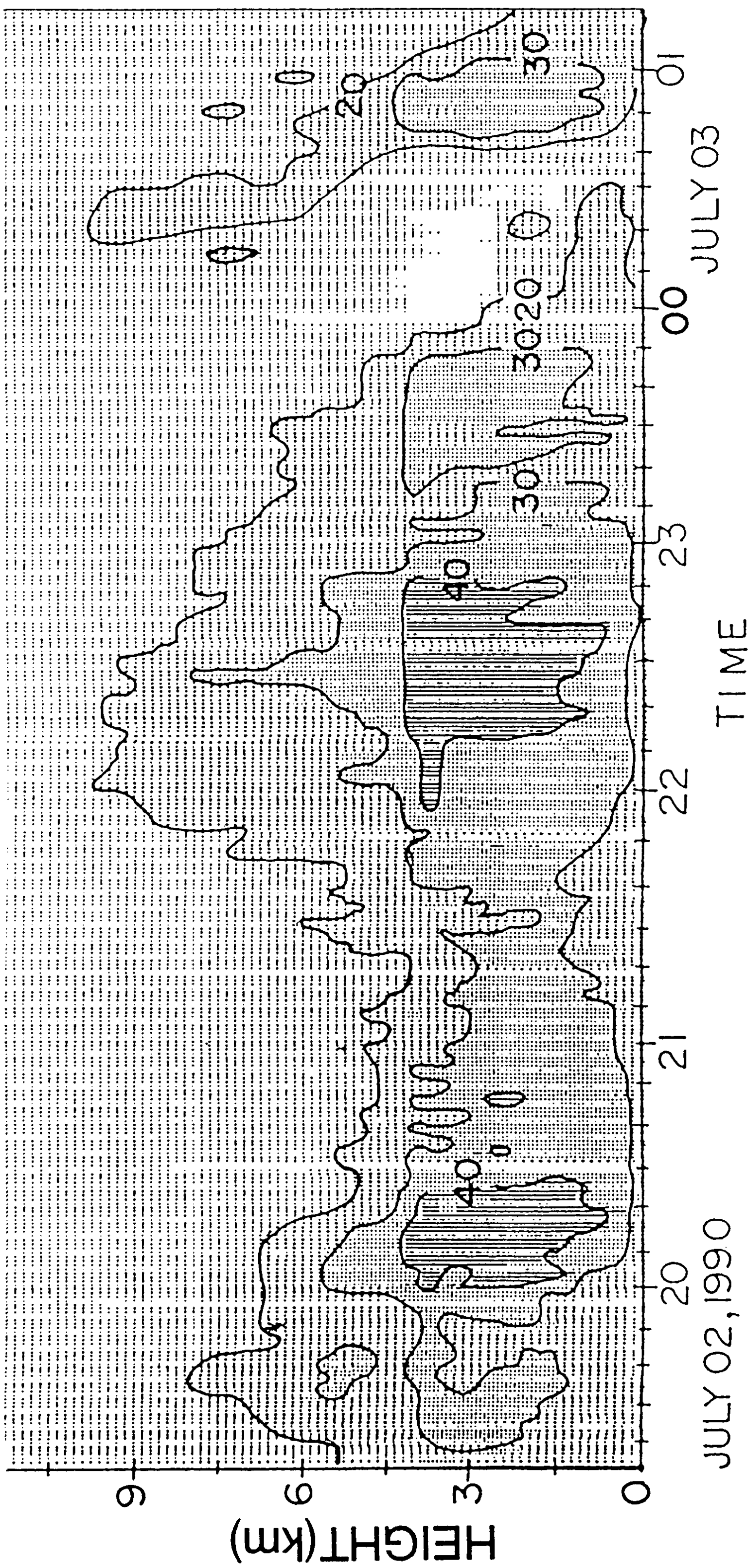

Fig. 7. Echo power observed by the Ku-band radar at the MU radar site (unit is dBZe) from 1915 JST on July 2 to 0115 JST on July 3, 1990.

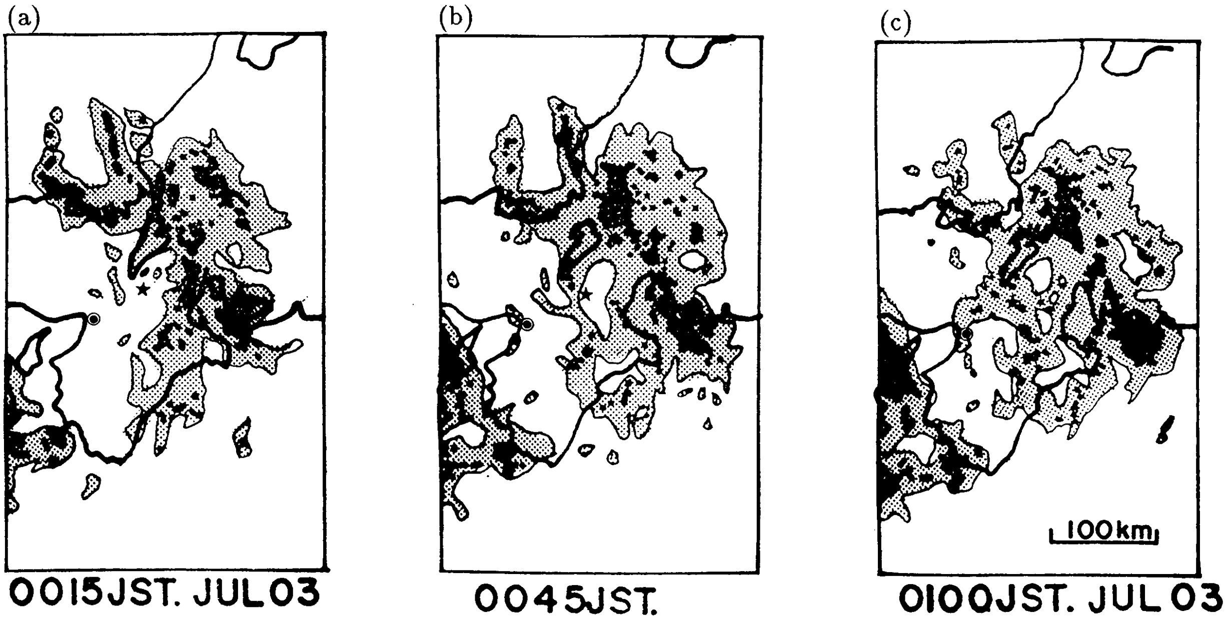

Fig. 8. Distribution of echo power observed by a standard meteorological radar (⊙) of the Osaka Meteorological Observatory (OMO) of JMA at (a) 0015 JST, (b) 0045 JST and (c) 0100 JST on July 3, 1990. The black region indicates rainfall between 1 and 4 mm/h, and the shaded region indicates rainfall less than 1 mm/h. The MU radar site is shown by a star.

ature observed by many weather stations belonging to OMO (see Fig. 9) indicate that the rotor appears in a meso-β-scale region where the surface pressure decreases more than 0.8 hPa/h. There is a region of temperature rise of more than 0.2 K/h to the west of or behind the center of the pressure depression (or trough). We note that the updraft portion of the rotor is located above the region of the surface temperature rise behind the surface pressure depression. The region of pressure depression moves eastward with a speed of ~50 km/h. This is consistent with the speed of the clear region observed by the OMO radar, and hence the rotor drift.

Figure 10 shows a schematic of the speculated three-dimensional structure of the rotor circulation observed here. The rotor forms over a meso-β-scale warm depression moving eastward. An updraft appears above and behind the rotor center, while a downdraft appears in front of it. Tall precipitating banded clouds develop just behind the rotor, and other banded clouds exist at a distance in front of the rotor. The rotor and the banded clouds are organized in a meso-α-scale cyclone-front system.

5. Discussions on the generation mechanism

As mentioned in Section 1, most of the rotor circulations studied earlier were associated with a large-amplitude mountain (or lee) wave developed by shear (or Kelvin-Helmholtz) instabilities (see, *e.g.*, Gerbier and Berenger, 1961). Generation of a rotor-like circulation pattern due to a plume (*e.g.*, Nakai, 1990) is rejected in the present case, since the planetary boundary layer is rather stable. So we must examine the effect of mountains and shear instability as plausible generation mechanisms of the rotor circulation observed here.

Stationary waves directly induced by mountains cannot be observed by a single-station observation such as the MU radar observation. However, based on the MU radar observations in the upper troposphere and in the lower stratosphere, K. Sato (1992) has suggested the frequent existence of mountain waves induced possibly in a southwestern part of the Japanese Archipelago, by considering a transience of the basic flow as the origin of a non-zero phase speed of those waves. The scale (~40 km × 150–200 km) and movement speed (~50 km/h) of the rotor observed here are not far from the horizontal wavelengths and phase speeds of mountain waves described in her study, so that this phenomenon might be associated with some lee waves developed locally by mountains around the MU radar observatory. We have not yet detected such a rotor, because most of those waves are not sufficiently developed as to generate it, and/or because they may be almost stationary in the lower troposphere. Therefore, we need much more explanation as to why some lee waves can develop to be large enough to generate the distinct rotor circulation in this case, and why they have non-zero phase speed even near the ground-level sources.

The simplest method to consider the development of mountain waves is to apply the classical shear instability theory for a two-layer fluid system, which

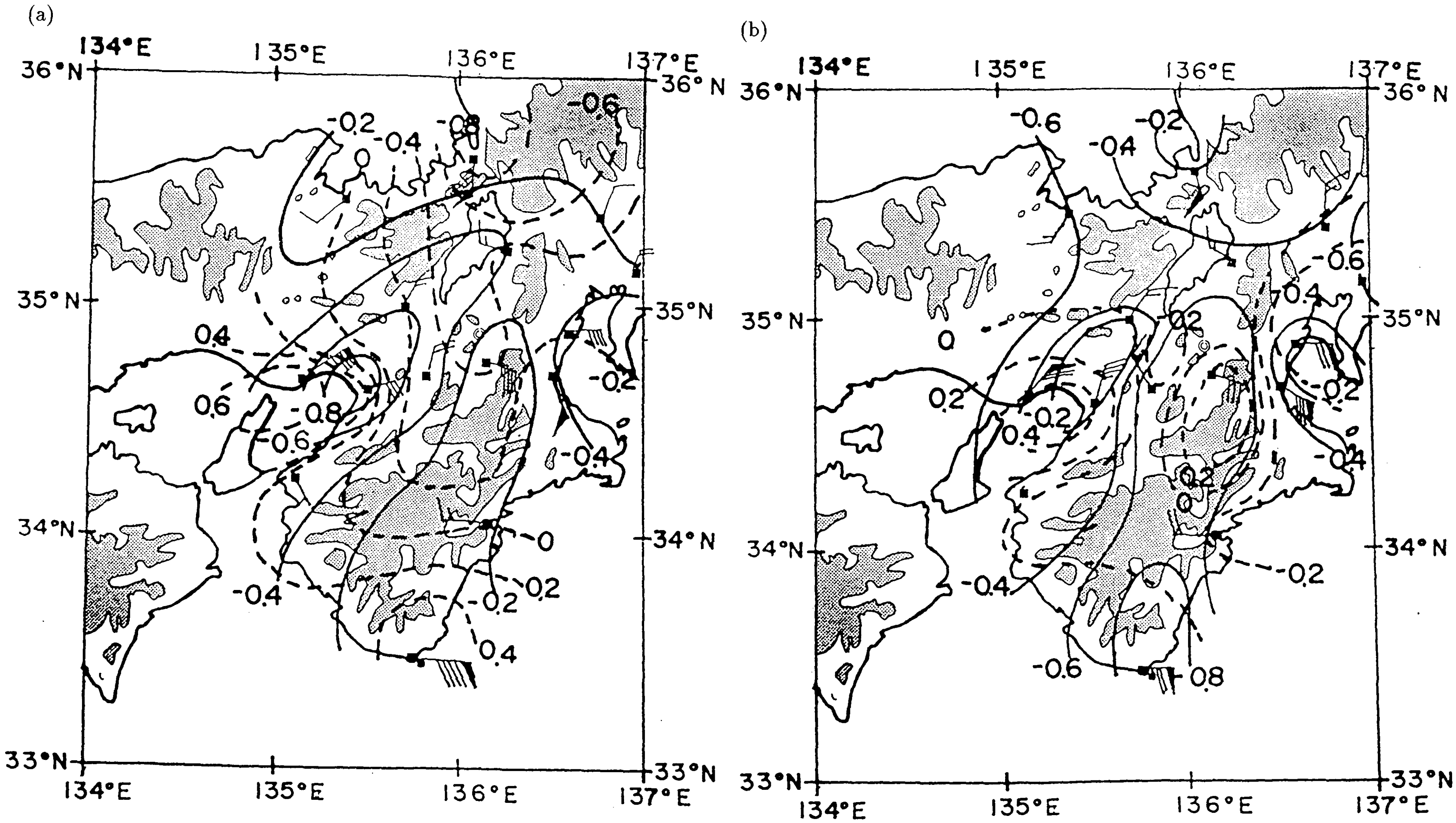

Fig. 9. Surface pressure (solid contours, every 0.2 hPa) and temperature (dashed contours, every 0.2°C) changes (a) from 23 JST on July 2 to 00 JST on July 3 and (b) during 00–01 JST on July 3 1990, analyzed from the routine meteorological data collected by OMO. Surface winds are also indicated by barbs (1 m/s) and pennants (5 m/s).

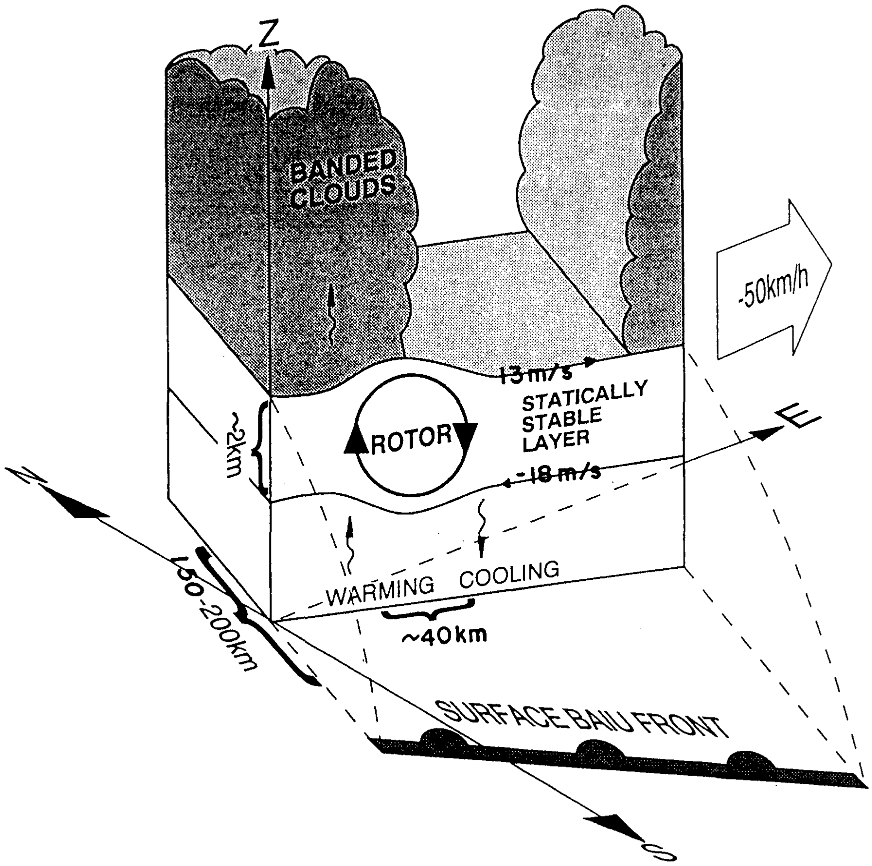

Fig. 10. Schematic structure of the rotor circulation observed in this study.

predicts that a wave generated in the boundary surface between the two layers has a horizontal wavelength given by

$$\lambda=\frac{2\pi}{g}\left[\frac{\overline{\Theta}}{\Delta\Theta}\left\{(c-\overline{U})^2+(\Delta U)^2\right\}+2\Delta U(c-\overline{U})\right],$$

where U and Θ are horizontal wind velocity and (equivalent) potential temperature in an *unperturbed* state, $\overline{(\ )}$ and $\Delta(\ )$ denote the average and half difference of values for the upper and lower layers, c is the horizontal phase velocity and g is the gravity acceleration. The wave is trapped in the vicinity of the interfacial surface and damped both upward and downward with a vertical scale of $\lambda/2\pi$. If we consider a thin layer in the vicinity of 2 km altitude and specify $U\approx-18$ m/s and $\Theta\approx 333$ K for the lower layer and $U\approx 13$ m/s and $\Theta\approx 339$ K for the upper layer from the observational results shown in Section 3, then we have $\overline{U}\approx-2.5$ m/s, $\Delta U\approx 15.5$ m/s, $\overline{\Theta}\approx 336$ K and $\Delta\Theta\approx 3$ K. We may specify $c\approx$ 15 m/s from Section 4. These specifications lead to $\lambda_c\approx 40$ km, which seems to be close to the size of the observed rotor but does not develop in time because $\lambda>\lambda_c$ (the longest unstable wavelength) $\approx$20 km in this case. If we consider a much thicker (thinner) layer and specify a larger (smaller) value for $\Delta\Theta$, then we obtain shorter (longer) values both for λ and for λ_c. It is shown in this simplest theory that we must specify $\Re c$ (the real part of c) $\approx\overline{U}$, which is, in general, smaller than the phase speed observed here, in order to obtain an unstable mode with $\lambda<\lambda_c$.

A more advanced treatment of the shear instability is to solve an eigenvalue problem of the Taylor-Goldstein (or Scorer, if $c=0$) equation with realistic continuous vertical profiles of Θ and U (*e.g.*, Takayabu, 1992). Then the Miles-Howard theorem, in general, states that $\Re c$ for an unstable mode must be bounded by the minimum and maximum values of U in the region where $Ri<1/4$ in an unperturbed state. However, we again encounter the difficulty on specifications for the unperturbed state, and obtain $\Re c$ smaller than the phase speed observed here, as long as we specify U with the profile actually observed in Section 3 including the very narrow layer of $Ri<1/4$.

Quasi-linear or non-linear numerical studies (*e.g.*, Tanaka, 1975; Klaassen and Peltier, 1985) have shown the time evolutions of Kelvin-Helmholtz billows including rotor circulations (or so-called cat's eye patterns). Then, the *mean* field is also changed in time from the initial unperturbed (or basic) state. Although the decay of billows is highly dependent on the microscale diffusion processes, maintenance of the mean field satisfying $Ri < 1/4$ is inevitably necessary for developing such billows. Namely, some suitable orographic or else sufficiently long-lasting atmospheric situations must exist to maintain the cat's eyes or rotor circulations. Indeed, as mentioned in the beginning of this section, mountains may be necessary to maintain this suitable situation. However, the movement speed of cat's eyes again becomes smaller than that of the rotor observed here, if the initial state is specified with the profile observed actually just before the rotor appeared.

The shear instability theories mentioned in the three paragraphs above do not include any contributions of dynamical processes other than and larger than an unstable wave itself. However, as mentioned in Section 4, the meso-β-scale horizontal structure of the rotor, as well as those of the banded clouds, is clearly defined by and organized in a meso-α-scale extra-tropical cyclone on the Baiu front. The situation $Ri < 1$ observed in a rather broader region near the rotor satisfies a necessary condition of the (conditional) symmetric instability. Saitoh and Tanaka (1987, 1988) have shown by a numerical experiment that the banded precipitating clouds near the Baiu front are governed by this type of instability. They consider mainly the formation of a statically unstable layer (or generating cells) in the middle troposphere, but show also that there is maintained a statically stable layer between the stratiform cloud layer (just above the frontal surface) and the (statically unstable) planetary boundary layer. In fact, Ri is positive but small due to strong vertical shear induced by cold and wet air just below the Baiu front (see Section 2). Banded clouds similar to the generating cells were actually observed in parallel with and just above the height region of the rotor circulation, as mentioned in Sections 3 and 4. The rotor circulation observed here seems to be generated in such a meso-β-scale statically stable region just below the Baiu-frontal surface controlled by a meso-α-scale symmetric instability.

We consider that the symmetric instability as a common feature of the Baiu-frontal atmosphere is responsible for the generation of the rotor circulation observed here, but still wonder why we could observe such a striking feature in this limiting case. The movement of the meso-β-scale structures, as well as the rotor circulation observed here, is similar to the low-level jet stream described in Section 2. It is not so extravagant to consider that such a structure may locally induce a shear instability region with $Ri < 1/4$, for example, when a minimum phase of Ri of this structure is passed over some suitable orographic situations. Once the shear instability appears, a rotor circulation may be developed in a similar manner as described in the theories mentioned earlier, and extended within the meso-β-scale structure. Following the movement of the minimum Ri phase of the meso-β-scale structure, the local shear instability region may be somewhat shifted within the scale of similar orographic conditions but become gradually dissolved. Although detailed examinations of this hypothesis are beyond the scope of this paper describing an observational finding, the coupling effect between the symmetric and shear instabilities may explain all the observational features described in Sections 2–4 without inconsistency.

6. Conclusion

We have reported the first direct observation of a rotor circulation made by the MU radar. The rotor was in parallel with banded clouds in the upper layer, and was associated with a meso-β-scale surface depression (or trough). All of them were organized in a meso-α-scale cyclone on the Baiu front. The rotor circulation itself is considered to be developed by shear instability with a scale smaller than meso-β (perhaps above a suitable orographic condition) inside a meso-β-scale weak statically stable region of which the generation and maintenance are controlled by a meso-α-scale (conditional) symmetric instability near the Baiu front. All the meso-α-scale, meso-β-scale and much smaller scale (perhaps orographic) conditions must be suitable in order to generate this striking phenomenon moving with a non-zero speed. This is why such a rotor circulation has never been detected by the MU radar observations, which were started in 1984.

The rotor circulation observed here may be interesting not only from a fluid-dynamical viewpoint but also as a Baiu-frontal phenomenon. Almost all the foregoing mesoscale observational studies on the Baiu front have treated statically-unstable precipitating phenomena based on the satellite cloud imageries or the microwave-radar raindrop echoes (*e.g.*, Ninomiya and Akiyama, 1974; Akiyama, 1978), whereas this study has revealed a statically-stable three-dimensional circulation based on the powerful MU radar technique (see also Fukao *et al.*, 1988; Kotani *et al.*, 1993; and references therein). The atmosphere is statically stable in most regions, even near the Baiu front. Although detailed discussions are beyond the scope of this paper, we believe that such a statically stable phenomenon is also important to understand mechanisms of the hierarchical structure formation in the Baiu-frontal atmosphere.

Acknowledgment

We thank Mr. G. Kotani for his processing of the original MU radar data used in this study, Drs. T. Sato, T. Tsuda, M. Yamamoto and T. Nakamura for their cooperation at the MU radar observatory, and Dr. W.L. Oliver, Jr. for his careful reading of the original manuscript. The Osaka Meteorological

Observatory kindly permitted us to use the data of meteorological radar and weather stations. The MU radar belongs to and is operated by the Radio Atmospheric Science Center of Kyoto University.

References

Akiyama, T., 1973: The large-scale aspects of the characteristic features of the Baiu front. *Pap. Meteor. Geophys.*, **24**, 157–158.

Akiyama, T., 1978: Mesoscale pulsation of convective rain in medium-scale disturbances developed in Baiu front. *J. Meteor. Soc. Jaban*, **56**, 267–283.

Bretherton, F.P., 1969: Momentum transport by gravity waves. *Quart. J. Roy. Meteor. Soc.*, **95**, 213–243.

Browning, K.A., M.E. Hardman, T.W. Harrold and C.W. Pardoe, 1973: The structure of rainbands within a mid-latitude depression. *Quart. J. Roy. Meteor. Soc.*, **99**, 215–231.

Förchtgött, J., 1949: Wave streaming in the lee of mountain ridges. *Bull. Meteor. Czech.*, **3**, 1–49.

Fukao, S., K. Wakasugi, T. Sato, T. Tsuda, I. Kimura, N. Takeuchi, M. Matsuo and S. Kato, 1985a: Simultaneous observation of precipitating atmosphere by VHF band and C/Ku band radars. *Radio Sci.*, **20**, 622–630.

Fukao, S., T. Sato, T. Tsuda, S. Kato, K. Wakasugi and T. Makihira, 1985b: The MU radar with an active phased array system, 1. Antenna and power amplifiers. *Radio Sci.*, **20**, 1155–1168.

Fukao, S., T. Tsuda, T. Sato, S. Kato, K. Wakasugi and T. Makihira, 1985c: The MU radar with an active phased array system, 2. In-house equipment. *Radio Sci.*, **20**, 1169–1176.

Fukao, S., M.D. Yamanaka, T. Sato, T. Tsuda and S. Kato, 1988: Three-dimensional air motions over the Baiu front observed by a VHF-band Doppler radar: A case study. *Mon. Wea. Rev.*, **116**, 281–292.

Fukao, S., M.D. Yamanaka, H. Matsumoto, T. Sato, T. Tsuda and S. Kato, 1989: Wind fluctuations near a cold vortex-tropopause funnel system observed by the MU radar. *Pure Appl. Geophys.*, **130**, 463–479.

Fukao, S., M.F. Larsen, M.D. Yamanaka, H. Furukawa, T. Tsuda and S. Kato, 1991: Observations of a reversal in long-term average vertical velocities near the jetstream wind maximum. *Mon. Wea. Rev.*, **119**, 1479–1489.

Gerbier, N. and M. Berenger, 1961: Experimental studies of lee waves in the French Alps. *Quart. J. Roy. Meteor. Soc.*, **87**, 13–23.

Hobbs, P.V., 1978: Organization and structure of clouds and precipitation on the mesoscale and microscale in cyclonic storms. *Rev. Geophys. Space Phys.*, **16**, 741–755.

Klaassen, G.P. and W.R. Peltier, 1985: Evolution of finite amplitude Kelvin-Helmholtz billows in two spatial dimensions. *J. Atmos. Sci.*, **42**, 1321–1339.

Kotani, G., M.D. Yamanaka, S. Fukao, T. Sato, M. Yamamoto, T. Tsuda and S. Kato, 1993: Medium-scale and mesoscale dynamical structures of the Baiu front observed by the MU Radar: A case study. *J. Meteor. Soc. Japan*, **71**, in press.

Larsen, M.F., S. Fukao, O. Aruga, M.D. Yamanaka, T. Tsuda and S. Kato, 1991: A comparison of VHF radar vertical velocity measurements by a direct vertical beam method and by a VAD technique. *J. Atmos. Ocean. Tech.*, **8**, 766–776.

Larsson, L., 1954: Observations of lee wave clouds in the Jamtland Mountains, Sweden. *Tellus*, **6**, 124–138.

Lilly, D.K., 1971: Observations of mountain-induced turbulence. *J. Geophys. Res.*, **76**, 6585–6588.

Matsumoto, S., K. Ninomiya and S. Yoshizumi, 1971: Characteristic features of Baiu front associated with heavy rainfall. *J. Meteor. Soc. Japan*, **49**, 267–281.

Matsuo, T. and Y. Sasyo, 1981: Melting of snowflakes below freezing level in the atmosphere. *J. Meteor. Soc. Japan*, **59**, 10–25.

May, P.T., S. Fukao, P.J. Neiman, M.W. Kozleski, M.D. Yamanaka, S. Kato, M. Yamamoto, T. Sato and T. Tsuda, 1992: MU radar observations of the wind field in the vicinity of the Baiu front during early July, 1987. *Beitr. Phys. Atmos.*, **65**, 3–11.

Nakai, M., 1990: Laboratory study on the behavior of pure plumes in stably stratified cross-flows. *J. Japan Soc. Fluid Mech.*, **9**, 262–271 (in Japanese).

Ninomiya, K. and T. Akiyama, 1974: Band structure of mesoscale echo cluster associated with low-level jet stream. *J. Meteor. Soc. Japan*, **52**, 300–313.

Palmer, R.D., M.F. Larsen, R.F. Woodman, S. Fukao, M. Yamamoto, T. Tsuda and S. Kato, 1991: VHF radar interferometry measurements of vertical velocity and the effect of tilted refractivity surfaces on standard Doppler measurements. *Radio Sci.*, **26**, 417–427.

Saitoh, S. and H. Tanaka, 1987: Numerical experiments of conditional symmetric baroclinic instability as a possible cause for frontal rainband formation, Part I: A basic experiment. *J. Meteor. Soc. Japan*, **65**, 675–708.

Saitoh, S. and H. Tanaka, 1988: Numerical experiments of conditional symmetric baroclinic instability as a possible cause for frontal rainband formation, Part II: Effects of water vapor supply. *J. Meteor. Soc. Japan*, **66**, 39–54.

Sato, K., 1990: Vertical wind disturbances in the troposphere and lower stratosphere observed by the MU radar. *J. Atmos. Sci.*, **47**, 2803–2817.

Sato, T., H. Doji, H. Iwai, I. Kimura, S. Fukao, M. Yamamoto, T. Tsuda and S. Kato, 1990: Computer processing for deriving drop-size distributions and vertical air velocities from VHF Doppler radar spectra. *Radio Sci.*, **25**, 961–973.

Takayabu, I., 1992: Kelvin-Helmholtz billow clouds on a frontal surface. *J. Meteor. Soc. Japan*, **70**, 733–738.

Takeda, T. and Y. Fujiyoshi, 1978: Micro-physical processes around melting layer in precipitating clouds as observed by vertically pointing radar. *J. Meteor. Soc. Japan*, **56**, 293–303.

Takeda, T. and M. Horiguchi, 1986: Simultaneous observation of fine structure of layer clouds at upper- and middle-levels by a laser radar and a 8.6 mm radar. *J. Meteor. Soc. Japan*, **64**, 109–122.

Tanaka, H., 1975: Quasilinear and nonlinear interactions of finite amplitude perturbations in a stably stratified fluid with hyperbolic tangent shear, *J. Meteor. Soc. Japan*, **53**, 1–31.

Wakasugi, K., A. Mizutani, M. Matsuo, S. Fukao and S. Kato, 1986: A direct method for deriving drop-size distribution and vertical air velocities from VHF Doppler radar spectra. *J. Atmos. Ocean. Tech.*, **3**, 623–629.

Yokoyama, T., H. Tanaka, K. Nakamura and J. Awaka, 1984: Microphysical processes of melting snowflakes detected by two-wavelength radar. Part II: Application of two-wavelength radar technique. *J. Meteor. Soc. Japan*, **62**, 668–678.

Yokoyama, T., H. Tanaka, K. Akaeda, T. Ohtani, N. Yoshizawa, M.D. Yamanaka, A. Mita, Y. Ishizaka and A. Ono, 1985: Observation on microphysical processes in the stratiform precipitations including melting layers at Mt. Fuji. *J. Meteor. Soc. Japan*, **63**, 100–111.

MU レーダーで観測された梅雨前線近傍のローター循環

渡辺　明
(福島大学教育学部)
深尾昌一郎・山中大学
(京都大学超高層電波研究センター)
住　明正
(東京大学気候システム研究センター)
上田　博
(北海道大学理学部)

MU レーダー (滋賀県信楽町) を用いた下部対流圏 3 次元風速ベクトルの連続ドップラー観測から、梅雨前線近傍に存在するローター循環を検出した。ここで報告するような顕著なものが、流れの鉛直成分を含めて現実に観測されたのは、筆者等の知る限りにおいてこれが初めてである。ローターの時間および鉛直スケールは約 50 分および約 2 km であり、また並行して行われたラジオゾンデ観測によれば、出現領域は静力学的に安定な成層構造をなしていた。気象庁高層観測および衛星観測に基く総観場および雲の解析から、ローターが出現した領域は梅雨前線面のすぐ下方であり、かつ中間 (メソα) 規模低気圧に伴って組織化されたバンド状降水雲の間に位置することがわかった。MU レーダーと同時に行った 2 周波 (C/Ku 帯) 気象レーダー観測で得られた降水粒子エコーは、ローター前面の下降流域では極めて弱く、後面の上昇流域では極めて顕著で約 9 km 高度にまで達していた。さらに大阪管区気象台によるレーダー観測およびメソ天気図解析から、このローターは、東西に約 40 km 、 南北に約 150~200 km の大きさを持ち東方へ時速約 50 km で進む中 (メソβ) 規模擾乱と同定された。成因について現時点で最も有力と考えられるのは、中間規模 (条件付) 対称不安定擾乱に伴って維持された弱い静力学的安定層中で、局所的シア不安定で偶発的に成長した中規模擾乱であるとするものである。